



# The Thermal and Settlement Characteristics of Crushed-Rock Structure Embankments of the Qinghai-Tibet Railway in Permafrost Regions Under Climate Warming

Qihang Mei<sup>1,2</sup>, Bin Yang<sup>3</sup>, Ji Chen<sup>1,2\*</sup>, Jingyi Zhao<sup>1,2</sup>, Xin Hou<sup>1,2</sup>, Youqian Liu<sup>4</sup>, Jinchang Wang<sup>4</sup>, Shouhong Zhang<sup>4</sup> and Haiming Dang<sup>4</sup>

## OPEN ACCESS

### Edited by:

Jing Luo,  
Northwest Institute of Eco-  
Environment and Resources (CAS),  
China

### Reviewed by:

Yinghong Qin,  
Guangxi University for Nationalities,  
China

Qing Wang,  
Jilin University, China

### \*Correspondence:

Ji Chen  
chenji@lzb.ac.cn

### Specialty section:

This article was submitted to  
Cryospheric Sciences,  
a section of the journal  
Frontiers in Earth Science

**Received:** 15 October 2021

**Accepted:** 22 November 2021

**Published:** 09 December 2021

### Citation:

Mei Q, Yang B, Chen J, Zhao J, Hou X,  
Liu Y, Wang J, Zhang S and Dang H  
(2021) The Thermal and Settlement  
Characteristics of Crushed-Rock  
Structure Embankments of the  
Qinghai-Tibet Railway in Permafrost  
Regions Under Climate Warming.  
*Front. Earth Sci.* 9:795894.  
doi: 10.3389/feart.2021.795894

<sup>1</sup>Beiluhe Observation and Research Station of Frozen Soil Engineering and Environment, State Key Laboratory of Frozen Soil Engineering, Northwest Institute of Eco-Environmental and Resources, Chinese Academy of Sciences, Lanzhou, China, <sup>2</sup>School of Engineering Science, University of Chinese Academy of Sciences, Beijing, China, <sup>3</sup>Command Center of Comprehensive Natural Resources Survey, China Geological Survey, Beijing, China, <sup>4</sup>China Railway Qinghai-Tibet Group Co., Ltd., Xining, China

The temperature difference at the top and bottom of the crushed-rock layer can drive the heat convection inside. Based on this mechanism, crushed-rock structures with different forms are widely used in the construction and maintenance of the Qinghai-Tibet Railway as cooling measures in permafrost regions. To explore the stability of different forms of crushed-rock structure embankments under climate warming, the temperature and deformation data of a U-shaped crushed-rock embankment (UCRE) and a crushed-rock revetment embankment (CRRE) are analysed. The variations in temperature indicate that permafrost beneath the natural sites and embankments is degrading but at different rates. The thermal regime of ground under the natural site is only affected by climate warming, while that under embankment is also affected by embankment construction and the cooling effect of the crushed-rock structure. These factors make shallow permafrost degradation beneath the embankments slower than that beneath the natural sites and deep permafrost degradation faster than that beneath the natural sites. Moreover, the convection occurring in the crushed-rock base layer during the cold season makes the degradation of permafrost beneath the UCRE slower than that in the CRRE. The faster degradation of permafrost causes the accumulated deformation of the CRRE to be far greater than that of the UCRE, which may exceed the allowable value of the design code. The analysis shows that the stability of the UCRE meets the engineering requirements and the CRRE needs to be strengthened in warm and ice-rich permafrost regions under climate warming.

**Keywords:** permafrost, crushed-rock structure embankment, stability, thermal regime, settlement

## INTRODUCTION

In recent decades, the thawing and disappearance of permafrost around the world caused by climate warming has challenged the stability of infrastructure located in cold regions (Nelson et al., 2011; Hong et al., 2014; Hjort et al., 2018; Karjalainen et al., 2019; Streletskiy et al., 2019). The Qinghai-Tibet Railway (QTR), a milestone project in a cold region, is located on the Qinghai-Tibetan Plateau (QTP) and crosses 550 km of continuous permafrost, of which 134 km is warm (with a mean annual ground temperature between 0 and  $-1^{\circ}\text{C}$ ) and ice-rich (with an ice content  $> 20\%$  by volume) permafrost (Wu et al., 2006; Zhang et al., 2008). On the QTP, the climate is warming faster than the global average, which makes its permafrost degenerate rapidly (Wu et al., 2015; Kuang and Jiao, 2016; Cheng et al., 2019; Ding et al., 2019). In warm and ice-rich permafrost regions, permafrost melting increases the risk of embankment instability, which makes it necessary to evaluate the embankment stability of the QTR over time (Wu et al., 2020a).

To stabilize the permafrost beneath the embankment, various proactive cooling measures, whose cooling effects have been verified in other projects, have been widely used in the construction of the QTR (Cheng, 2005; Cheng et al., 2009; Ma et al., 2009). Among these measures, crushed-rock embankments are the most widely used and have a total length of more than 150 km in the initial construction phase of the QTR (Mu, 2012). The common forms of crushed-rock embankment in permafrost regions include crushed-rock revetment embankments (CRREs), crushed-rock base embankments and U-shaped crushed-rock embankments (UCREs) formed by the combination of the former two (Mu et al., 2010). After 2006, a large number of traditional embankments and crushed-rock base embankments became CRREs and UCREs, respectively, after strengthening with crushed-rock revetment (Ma et al., 2012; Hou et al., 2015; Mu et al., 2018; Mei et al., 2021). The working mechanism of crushed-rock structures includes two parts: the cooling effect and insulation effect. The cooling effect occurs in the cold season when there is gravity induced convection between the cold air at the top of the crushed-rock layer and the warm air at the bottom by gravity (Goering and Kumar, 1996; Goering, 2003). The insulation effect occurs in the warm season when the air is stable and no convection heat exchange occurs inside the crushed-rock layer (Cheng et al., 2007). Monitoring data has revealed that the effective thermal conductivity of the crushed-rock layer in winter is 12.2 times that in summer (He et al., 2000). The change of thermal conductivity of the crushed-rock layer makes the embankment in a state of heat loss, which is beneficial to the cooling of permafrost.

The adaptability of crushed-rock embankments with different forms to climate warming has been studied by various methods. Analysis of the monitoring data of the QTR shows that crushed-rock structures can slow down the warming of permafrost and the deformation of embankments, and the cooling effect is related to the mean annual ground temperature (MAGT) (Ma et al., 2008a; Wu et al., 2008; Luo et al., 2018; Mu et al., 2018). There are differences in the stability of crushed-rock embankments with different forms, among which UCREs have the best stability and

CRREs have the worst stability (Niu et al., 2015; Zhao et al., 2019; Wu et al., 2020b; Tai et al., 2020). In addition, through the establishment of mathematical model, Lai et al. (2003, 2006, 2014) analysed the embankment stability of the QTR with air temperature increases of 2.0 and  $2.6^{\circ}\text{C}$  in the next half century, and the results showed that crushed-rock base embankments could remain stable under such climate warming conditions.

In the warm permafrost regions, the permafrost is more prone to degradation, which results in the cooling effect of the crushed-rock structures being different from that of general permafrost areas. However, the research of the stability of crushed-rock embankment with different forms and the reasons for the difference in cooling effect of these structures are still insufficient under climate change. Therefore, this paper analyses the sources of embankment deformation under climate change by combining ground temperature and ice content at different depths of permafrost. And by analysing the change of heat flow, the reasons for the difference of cooling effect between the two crushed-rock structures are studied. The results of this study can provide a reference for the selection of cooling measures in the construction and maintenance of other projects.

## DATA AND METHODS

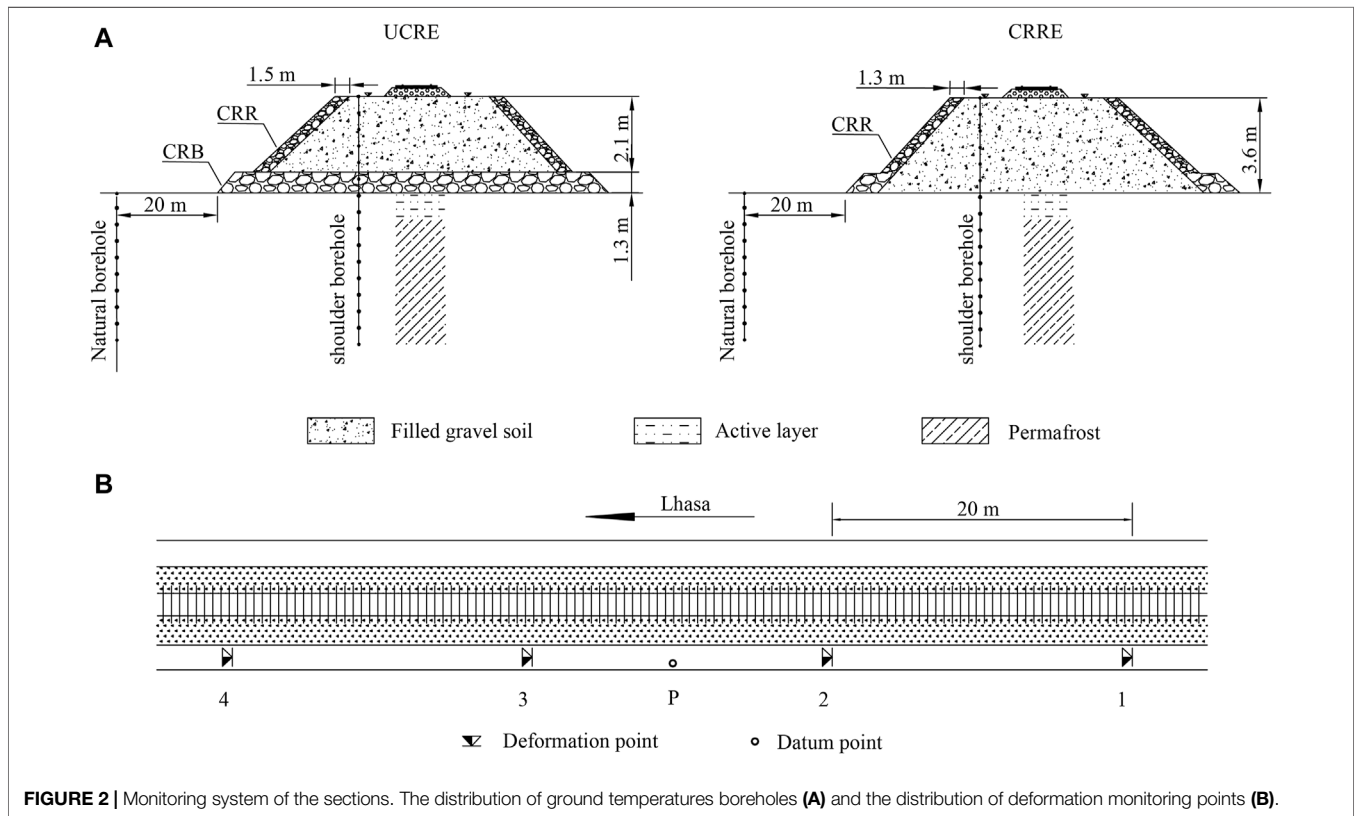
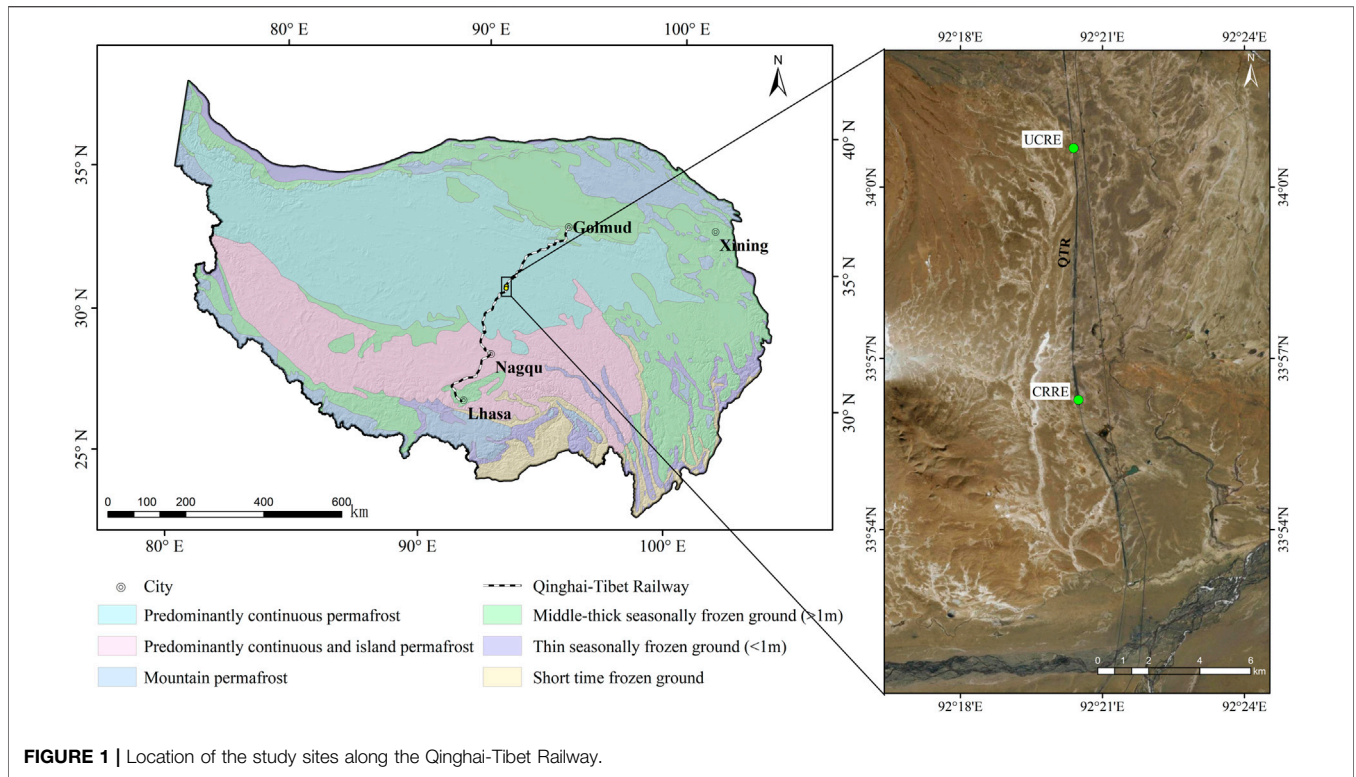
### Site Description

The UCRE and CRRE sections along the QTR in this study are located in the Kaixinling Mountain region of the QTP, with altitudes of 4,672 m and 4,622 m, respectively (Figure 1). The study area is a continuous permafrost area. The temperature data from the Kaixinling Weather Station in the last 5 years (2014–2018) show that the mean annual air temperature is between  $-3.29$  and  $-4^{\circ}\text{C}$ , and the mean daily temperature drops below  $0^{\circ}\text{C}$  from September to May during the next year.

Both the UCRE and CRRE were constructed in phases during the warm seasons of 2002 and 2003, with heights of 3.4 and 3.6 m, respectively (Figure 2A). The revetment thicknesses of the UCRE and CRRE are 1.5 and 1.3 m, respectively, and they are composed of crushed rock with diameters of approximately 10 cm. The crushed-rock base layer of the UCRE is 1.3 m thick and consists of crushed rock with diameters of approximately 35 cm. Borehole drilling conducted in 2004 revealed the permafrost table (PT) depth of the natural sites around the UCRE and CRRE were 2.4 and 3.4 m, respectively. Several meters of ice content permafrost (with a volumetric ice content  $> 30\%$ ) were present under the PT. The ground temperatures at a depth of 15 m at the natural sites were  $-0.74$  and  $-0.80^{\circ}\text{C}$ , indicating that the UCRE and CRRE sections are located in warm permafrost regions. The orientations of the UCRE and CRRE are  $174^{\circ}$  and  $170^{\circ}$ , respectively, both of which are oriented approximately north to south.

### Monitoring Program

The thermal regime and deformation monitoring systems were established on the UCRE and CRRE sections and began operations at the end of 2005 (Ma et al., 2005). The thermal regime monitoring system for each section consisted of a 16 m



deep natural borehole outside the embankment area and a 20 m deep shoulder borehole located on the left shoulder (the left is defined in accordance with the direction from Golmud to Lhasa), as shown in **Figure 2A**. The temperature of the natural borehole is not affected by the construction and operation of the railway because it is 20 m from the left slope toe of the embankment (Wu et al., 2015). In this study, the monitoring temperature data of the natural borehole are used to reflect the impact of climate warming on the ground temperature. Thermistors with an accuracy of  $\pm 0.05^\circ\text{C}$  in the borehole were distributed at 0.5 m intervals from the surface to a depth of 10 m and at 1 m intervals below a depth of 10 m. The ground temperature was automatically measured once a day by a DT500 data logger.

The embankment deformation monitoring system consists of four deformation points (point 1 to point 4) and one datum point (point P), as shown in **Figure 2B**. The four deformation points are marked on the top of four steel spikes 20 m apart buried on the left shoulder. The elevation of these four points varies with the deformation of the embankment surface. The top of a steel pipe with a buried depth of 20 m was marked as the datum point which did not move with the deformation of the embankment. The embankment deformation is obtained by averaging four deformation points. The deformation is measured manually once a month by an optical level. The ground temperature and deformation data analysed in this paper are from 2006 to 2018. The damage to the instrument caused by the harsh natural environment makes part of the ground temperature data missing. From May to December 2009, the ground temperature data under the left shoulder of the UCRE was missing. From January to May 2007 and October to December 2008, the ground temperature under the left shoulder of the CRRE was missing. In the analysis, interpolation method was used to recover the missing ground temperature as much as possible. In addition, the interruption of manual observations caused the lack of data on the deformation of the embankment from January to April 2017.

## Methods

In this paper, the thermal regime of the embankments and natural sites is analysed by the MAGT, PT and ground temperature at different depths. The MAGT is defined as the temperature of soil or rock at a depth of zero annual amplitude of ground temperatures, which generally ranges from 10 to 20 m in the QTP (Jin et al., 2008). In the following analysis, the ground temperature at a depth of 15 m was selected as the MAGT. Based on the daily ground temperature, the PT beneath the natural sites and artificial permafrost table (APT) beneath the embankments were estimated by linear interpolation of the two adjacent depths of the  $0^\circ\text{C}$  isotherm. The terms heat flux and heat budget are introduced to characterize the thermal processes of the permafrost layer. The APT of the UCRE and CRRE is close to 5 m, so the heat flux  $q$  between 5.0 and 5.5 m is calculated using the following equation in this study:

$$q = -\lambda \frac{\partial T}{\partial z} \approx -\lambda \left( \frac{T_a - T_b}{\Delta z} \right) \quad (1)$$

where  $\lambda$  is the thermal conductivity of the soil. According to the soil type and ice content,  $\lambda$  equals  $1.08 \text{ W}\cdot\text{m}^{-1}\cdot\text{K}^{-1}$  in this equation (Xu et al., 2010).  $\Delta z$  equals 0.5 m, which is the thickness of the soil layer calculated.  $T$  is the soil temperature, where  $a$  and  $b$  are 5.5 and 5.0 m respectively. The heat budget is obtained by integrating the heat flux over time.

## RESULTS

### Permafrost Change at the Natural Sites

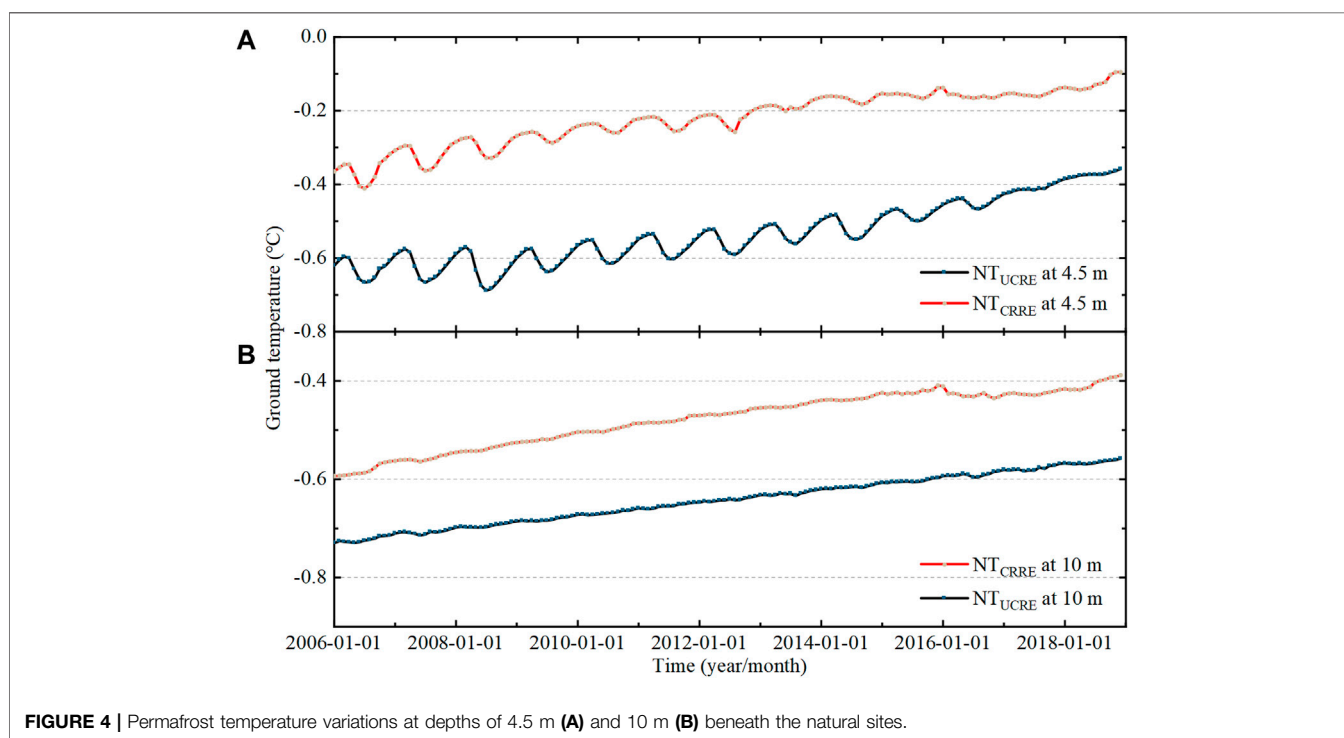
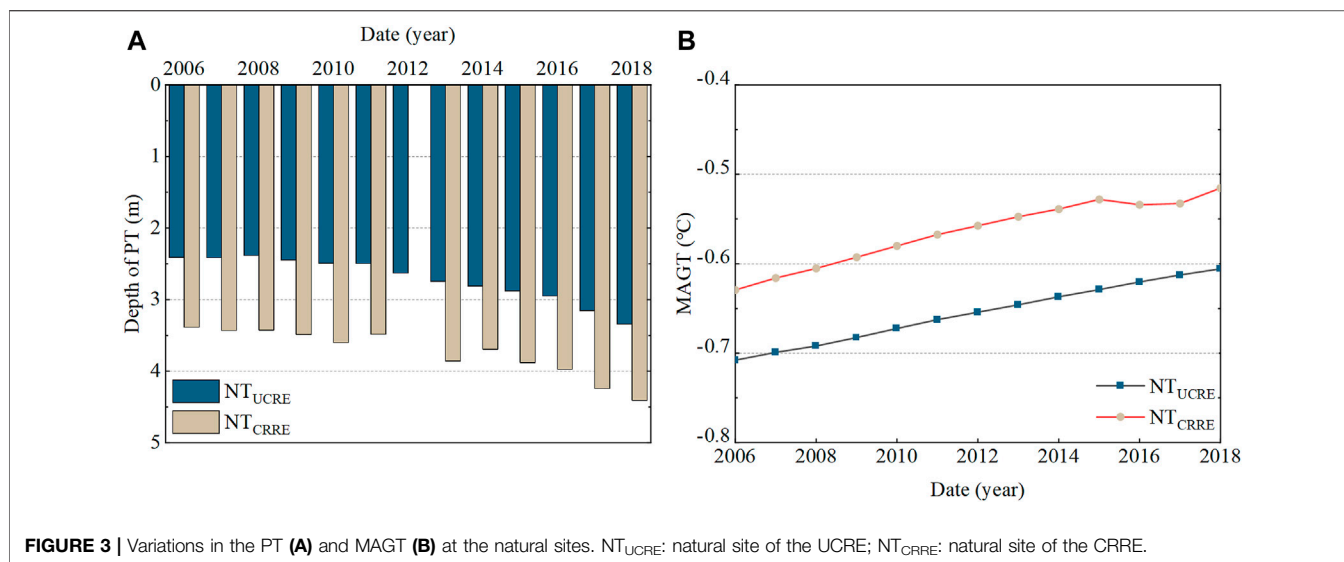
As shown in **Figure 3A**, the depth of the PT at the natural sites of UCRE and CRRE increased from 2.41 and 3.39 m to 3.34 and 4.41 m respectively, from 2006 to 2018. The ranges of increase of the two are close, 0.93 and 1.02 m, respectively. From 2006 to 2018, the MAGT beneath the two natural sites increased by 0.10 and  $0.11^\circ\text{C}$ , respectively (**Figure 3B**). The variation of PT depth and the MAGT indicates that the permafrost of the two natural sites is degrading at a basically uniform rate.

To study the degradation characteristics of permafrost beneath the natural sites in detail, the ground temperature of shallow permafrost (4.5 m) and deep permafrost (10 m) is selected for analysis, as shown in **Figure 4**. It is obviously that from 2006 to 2018, both shallow and deep permafrost beneath the natural sites of the UCRE and CRRE has been warming. At a depth of 4.5 m, the ground temperature fluctuated significantly with the seasons, and the mean annual temperatures of the UCRE and CRRE increased by  $0.26$  and  $0.27^\circ\text{C}$ , respectively (**Figure 4A**). In the deep of the permafrost (10 m), the temperature did not change with the seasons, and the mean annual temperature increased by  $0.17$  and  $0.21^\circ\text{C}$ , respectively (**Figure 4B**).

### Thermal Regime of the Embankments

Variations of the isotherms of the left shoulder indicate that there are significant differences in their thermal regimes beneath the UCRE and CRRE from 2006 to 2018, as shown in **Figure 5**. For example, in the first 5 years (2006–2011), the  $-0.4^\circ\text{C}$  isotherm beneath the UCRE remained stable at a depth of approximately 8 m (**Figure 5A**). Since 2012, the  $-0.4^\circ\text{C}$  isotherm has risen significantly, especially during the freezing period. After 2016, the isotherm began to decline and reached 8.7 m in 2018. However, the  $-0.4^\circ\text{C}$  isotherm beneath the CRRE declined uniformly from 7.8 m in 2006 to 9.8 m in 2018, a much larger decrease than that of the UCRE (**Figure 5B**). This phenomenon means that permafrost warming beneath the CRRE is faster than that beneath the UCRE. The APT beneath the embankment of both structures is lower than the original natural ground surface (the horizontal dotted lines in the figure). In addition, the variation in the APT beneath the embankment is staged, which is different from the variation in the PT beneath the natural sites.

As shown in **Figure 6A** with more detail, the variation in the APT beneath the UCRE and CRRE from 2006 to 2018 included three different stages. In the beginning, the APT beneath the embankment rose rapidly, but the duration and rise rate of the two embankments were different. The APT beneath the UCRE rose at a rate of  $0.35 \text{ m/a}$  from 2006 to 2008, while the APT



beneath the CRRE rose at a rate of 0.16 m/a from 2006 to 2011. The second stage was the stable period of the APT with a rate of change of less than 0.05 m/a. The durations of the UCRE and CRRE were 2008–2015 and 2011–2015, respectively. Since 2016, the APT beneath the UCRE and CRRE began to decline, with rates of 0.14 and 0.18 m/a, respectively. Overall, from 2006 to 2018, the APT beneath the UCRE rose by 0.5 m while that of the CRRE rose by 0.14 m.

The variation in the MAGT, which is closely related to the stability of permafrost, is shown in **Figure 6B**. From 2006 to 2018,

the MAGT of both embankment structures increased, but the rate of increase beneath the UCRE was lower than that beneath the CRRE. In 2006, the MAGT beneath the UCRE was higher than that of the CRRE, which was  $-0.7$  and  $-0.78^{\circ}\text{C}$ , respectively. However, as permafrost has been warming at different rates, the MAGT beneath the UCRE has been lower than that beneath the CRRE since 2014, and in 2018, it was  $-0.56$  and  $-0.54^{\circ}\text{C}$ , respectively.

To explore the thermal regime differences between the UCRE and CRRE, the ground temperatures at depths of 1.5 and 4 m

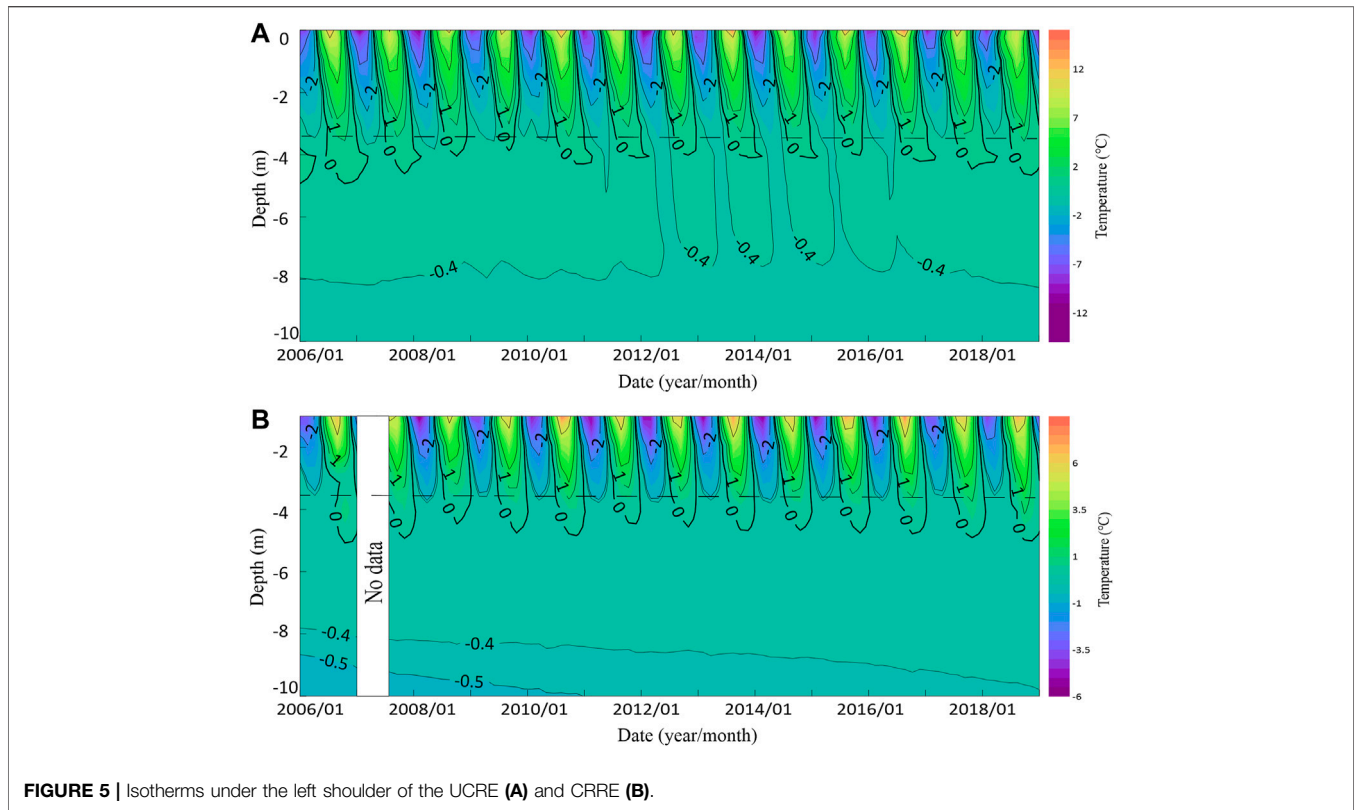


**FIGURE 5 |** Isotherms under the left shoulder of the UCRE (A) and CRRE (B).

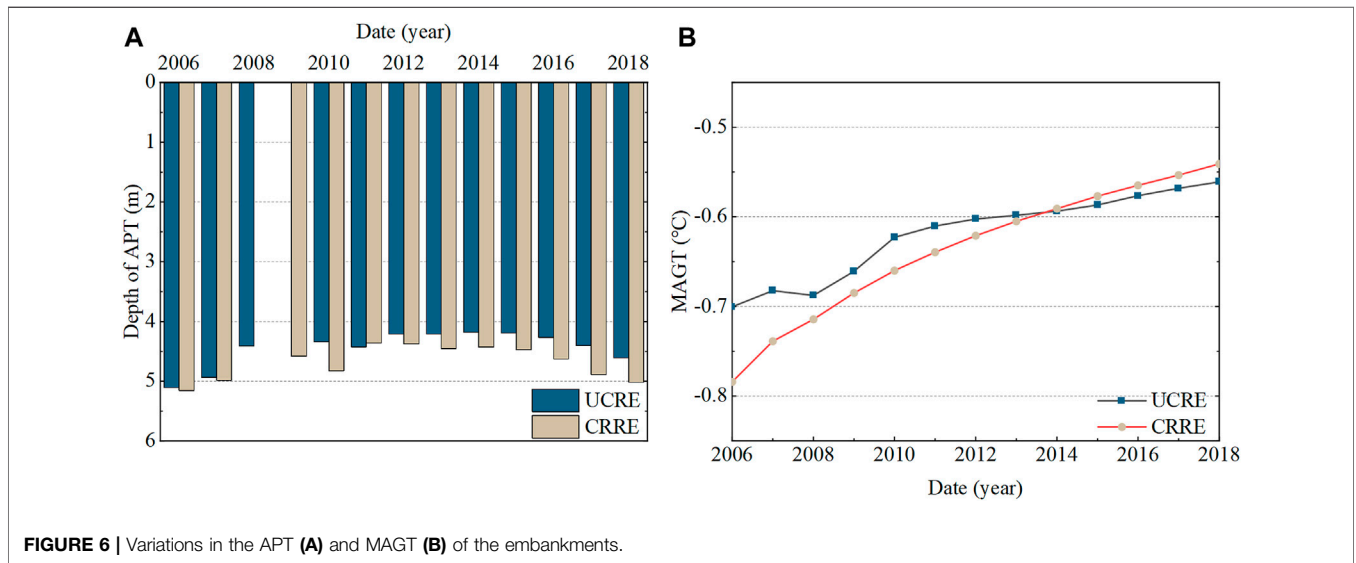


**FIGURE 6 |** Variations in the APT (A) and MAGT (B) of the embankments.

(corresponding to the top and bottom of the crushed-rock base in the UCRE, respectively) of the two embankments are analysed, as shown in **Figure 7**. At a depth of 1.5 m, the mean annual warming rate of both embankment sections from 2006 to 2018 is the same, which is  $0.17^{\circ}\text{C}/\text{a}$  (**Figure 7A**). Moreover, the annual range of ground temperature of the two embankments at this depth was basically the same. However, there are differences between the UCRE and CRRE at 4 m depth (**Figure 7B**). For the UCRE, the

ground temperature in the warm season stabilized at approximately  $0^{\circ}\text{C}$ . The ground temperature variation in the cold season can be divided into a decreasing stage (2006–2012) and an increasing stage (2012–2018). The annual minimum ground temperature decreased from  $-0.02$  to  $-0.78^{\circ}\text{C}$  in the first stage and then increased to  $-0.12^{\circ}\text{C}$  in the second stage. For the CRRE, the variation in ground temperature in the warm season can also be divided into two stages. The first stage was

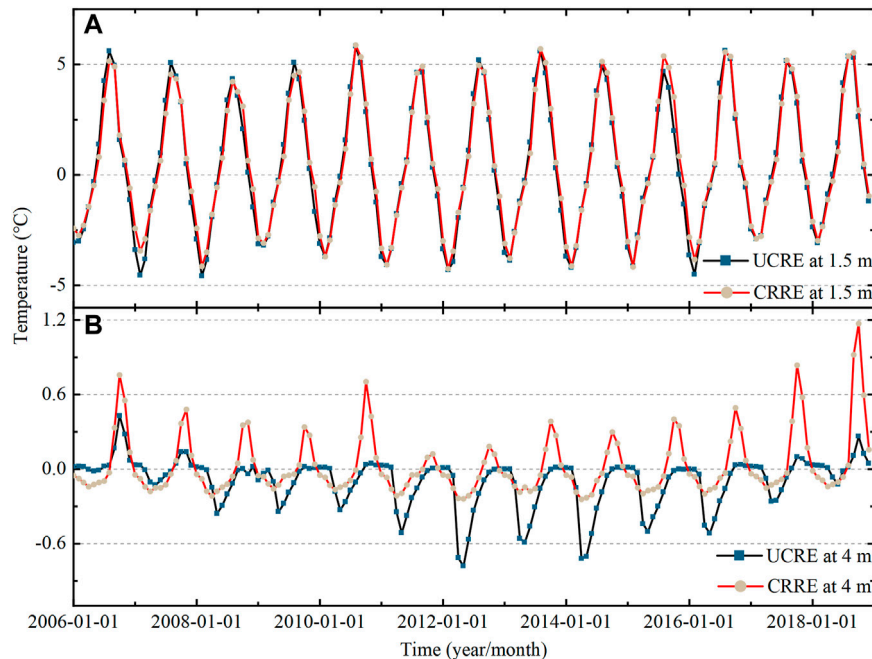


**FIGURE 7** | Ground temperature variations of the active layer at depths of 1.5 m **(A)** and 4 m **(B)** beneath the left shoulder of the embankments.

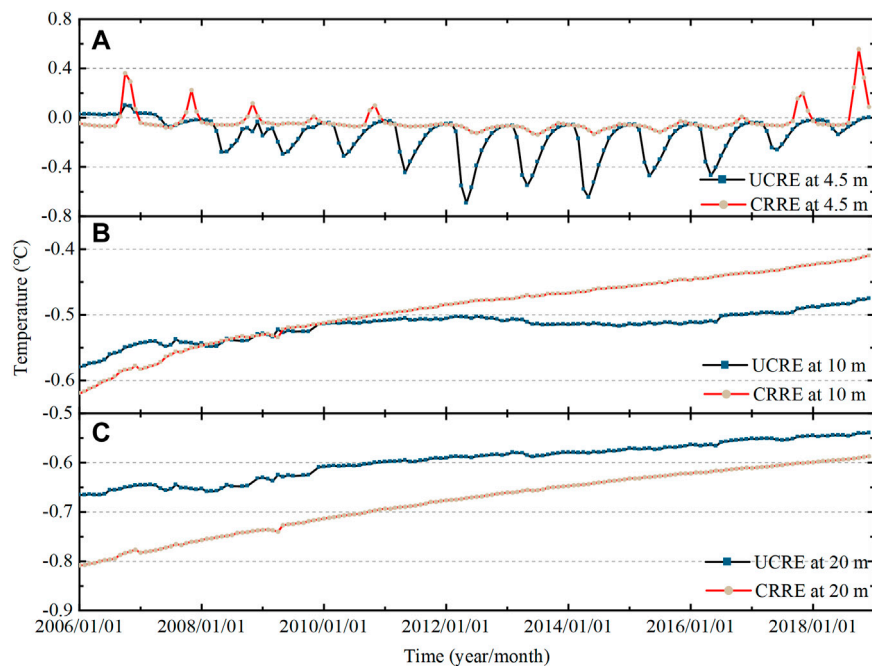


**FIGURE 8** | Permafrost temperature variations at depths of 4.5 m **(A)**, 10 m **(B)** and 20 m **(C)** beneath the left shoulder of the embankments.

from 2006 to 2011, when the annual maximum ground temperature decreased from 0.76 to 0.12°C. During the second period from 2011 to 2018, the annual maximum temperature increased from 0.12 to 1.17°C. In the cold season, the ground

temperature of the CRRE ranged from  $-0.14$  to  $-0.24^{\circ}\text{C}$ . It is obvious that in both the warm and cold seasons, the ground of the CRRE is warmer than that of the UCRE at a depth of 4 m.

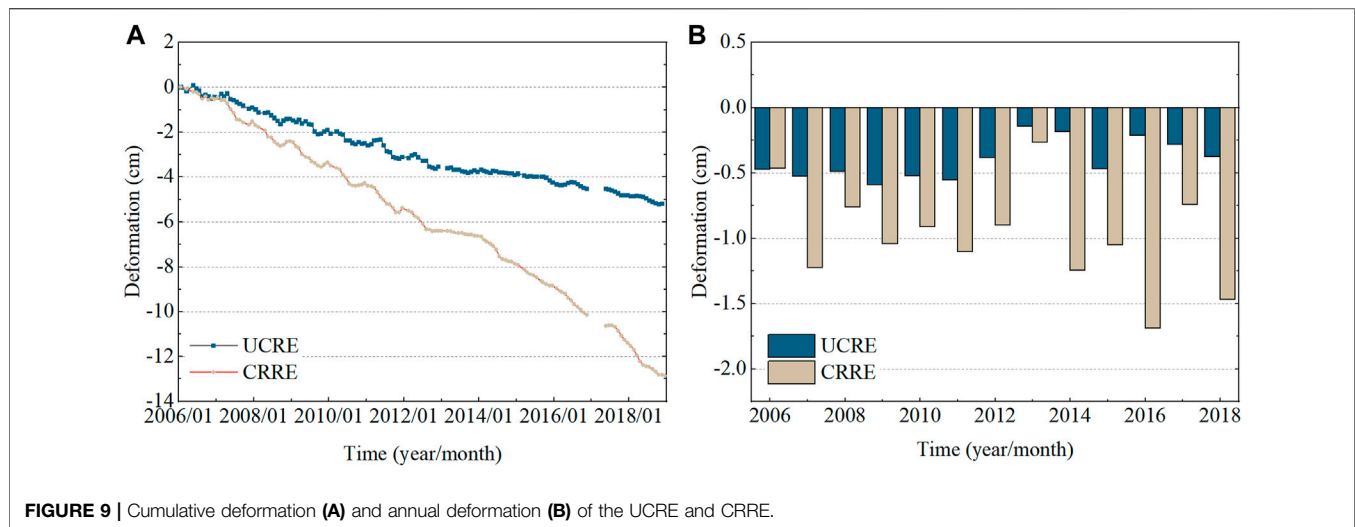


Figure 8 shows the variations of ground temperature within the permafrost layer beneath the UCRE and CRRE. Near the APT (4.5 m depth), the ground temperature of the UCRE in warm season and CRRE in cold season is basically stable, ranging from  $-0.15$  to  $0^{\circ}\text{C}$  (Figure 8A). However, the changes of ground temperature of the UCRE in cold season and CRRE in warm season are similar to those at 4 m, which decrease and increase in stages. From 2006 to 2018, the permafrost warming range of the UCRE and CRRE at a depth of 8 m was  $-0.10$  and  $-0.21^{\circ}\text{C}$ , respectively (Figure 8B). The warming rate of permafrost beneath the CRRE is  $0.016^{\circ}\text{C}/\text{a}$ , while the warming rate of the UCRE varied in three stages. During the initial 4 years (2006–2009), the permafrost in the UCRE warmed at a rate of  $0.016^{\circ}\text{C}/\text{a}$ , similar to that of the CRRE. In the second stage (2009–2016), the warming rate decreased to almost  $0^{\circ}\text{C}/\text{a}$ . After 2016, the warming rate increased to  $0.013^{\circ}\text{C}/\text{a}$ . At a depth of 20 m, the permafrost temperature of the UCRE and CRRE increased by  $0.12$  and  $0.22^{\circ}\text{C}$ , respectively. The above comparison of ground temperature at different depths shows that the permafrost warming of the CRRE is significantly faster than that of the UCRE in both warm and cold seasons.

## Embankment Deformation

Figure 9 shows the cumulative and annual deformation of the two embankment surfaces from 2006 to 2018. The settlement deformation of the UCRE and CRRE reached 5.2 and 12.9 cm, respectively, in 2018 (Figure 9A). The annual deformation of the two structural embankments was settlement deformation during the observation period. The maximum annual deformation of the UCRE was 0.59 cm in 2009. Since 2016, the mean annual deformation of the UCRE has been less than 0.3 cm, which is smaller than the previous value (Figure 9B). However, the annual deformation of the CRRE varies greatly, with maximum and minimum values of 1.7 cm in 2016 and 0.3 cm in 2013, respectively. Since 2016, the mean annual deformation of the CRRE has been 1.3 cm, which is much larger than that of the UCRE in the same period.

## DISCUSSION

### Thermal Stability of Permafrost Beneath Natural Sites and Embankments

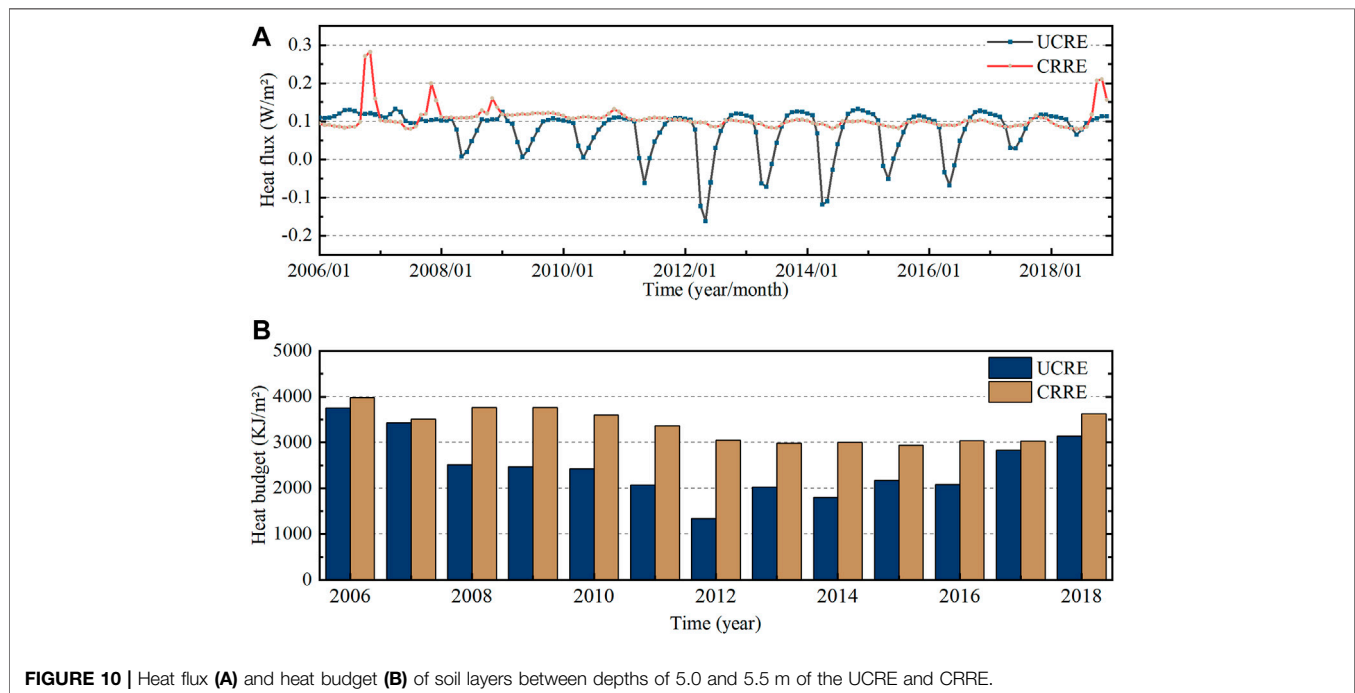
Previous studies show that under warming climate, the mean increase rate of the PT depth, ground temperature at a depth of 10 m and the MAGT beneath the natural sites along the QTR is 6.3 cm/a,  $0.015$  and  $0.012^{\circ}\text{C}/\text{a}$ , respectively (Wu et al., 2012; Zhang et al., 2020). Affected by local factors, the change rate of the PT beneath the natural sites in the study area is slightly greater than average, while the change rate of ground temperature at 10 and 15 m depth is smaller than average (Table 1). However, the stability of the permafrost beneath embankments is affected not only by climate warming but also by engineering activities. Engineering activities accelerate the degradation of permafrost beneath the embankment by changing the energy balance and moisture regimes (Tong and Wu, 1996; Wu et al., 2003; Jin et al., 2008; Peng et al., 2015; Ma et al., 2019).

In the two sections studied, the ground temperature data indicated the crushed-rock structure slowed down the warming of permafrost caused by climate warming and human activities. The PT beneath the two natural sites declined, while the APT beneath the two embankments rose, indicating that the thermal stability of the shallow permafrost beneath the embankment is better than that of the natural site, which can also be proven by the ground temperature change rate at a depth of 4.5 m. However, the cooling effect of the crushed-rock structure is gradually weakened with the long-term impact of climate change, which is the reason why the change rates of the APT and ground temperature at 4 m, 4.5 and 10 m are divided into stages, as shown in Figures 6–8 (Wu et al., 2007; Wu and Niu, 2013). The warming rates of permafrost at a depth of 15 m reveal that the deep permafrost beneath the embankment, especially beneath the CRRE, warms faster than the natural sites. The analysis shows that the cooling effect of the crushed-rock structures on the embankment mainly occurs in the shallow permafrost. The rise of the APT beneath the

**TABLE 1** | Rate of change in the (A)PT and ground temperature at different depths beneath natural sites and embankment from 2006 to 2018.

Site	Rate of change in (A)PT (cm/a)	Rate of change in permafrost temperature (°C/a)		
		4.5 m	10 m	15 m (MAGT)
NT <sub>UCRE</sub>	7.2	0.020	0.013	0.008
NT <sub>CRRE</sub>	7.8	0.021	0.016	0.009
UCRE	-3.8 <sup>a</sup>	0.002	0.008	0.012
CRRE	-1.0 <sup>a</sup>	0.010	0.016	0.021

<sup>a</sup>Negative values represent rising of APT.

**FIGURE 10** | Heat flux (A) and heat budget (B) of soil layers between depths of 5.0 and 5.5 m of the UCRE and CRRE.

embankment consumes the cold storage of the lower permafrost and causes the deep permafrost to warm up (Liu et al., 2019).

## Differences in the UCRE and CRRE Cooling Mechanisms

At a depth of 1.5 m, the ground temperature beneath the UCRE and CRRE is only affected by the revetment structure and upper soil, so their annual ranges of temperature and warming rate are the same. At a depth of 4 m, the crushed-rock base causes the ground temperature beneath the UCRE to be lower. In the warm season, the crushed-rock base isolates the lower soil to absorb heat from the upper layer. And in the cold season, the natural convection caused by temperature differences and the forced convection caused by wind in the crushed-rock base layer can effectively release heat from the lower soil. The cooling process in the active layer inevitably affects the thermal regime of the permafrost. The heat fluxes near the APT are shown in **Figure 10A**. The positive heat flow beneath the CRRE indicates that the permafrost is always in an endothermic

state. The heat flux beneath the UCRE is similar to that of the CRRE during the warm season. Since 2006, the amount of heat absorbed by the UCRE in the cold season has been gradually less than that by the CRRE as the cooling effect of the crushed-rock base layer has appeared, and the exothermic process has been present since 2011. However, the continuous warming of climate gradually weakens the convection in the crushed-rock base layer. As the cooling ability of the crushed-rock base layer decreases, the amount of heat absorbed by the UCRE in the cold season increases yearly, and the exothermic process of the UCRE disappeared after 2015. The convection that occurs in the crushed-rock base layer in the cold season causes the heat budget of the permafrost beneath the UCRE to be less than that beneath the CRRE in each freeze-thaw cycle (**Figure 10B**). The analysis of heat flux and heat budget shows that in the warm season, the thermal stability of permafrost beneath the UCRE and CRRE is similar, and the convection that occurs in the crushed-rock base layer makes the UCRE have a stronger cooling ability in the cold season. However, the long-term effect of climate warming causes the cooling effect difference between the UCRE and CRRE to gradually decrease after 2012.

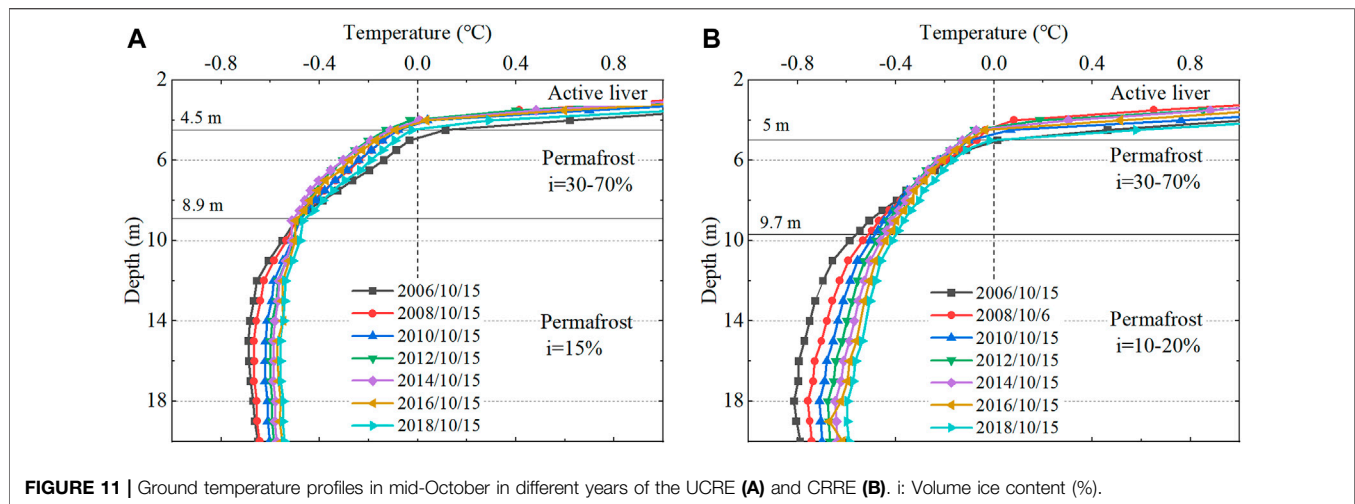


**FIGURE 11** | Ground temperature profiles in mid-October in different years of the UCRE (A) and CRRE (B): *i*: Volume ice content (%).

## Deformation Characteristics of the Embankments

Based on the long-term monitoring, it is found that the embankment deformation of the QTR is dominated by settlement deformation (Zhang et al., 2007; Ma et al., 2008b; Sun et al., 2018). According to the location of occurrence, the sources of embankment settlement in permafrost regions are divided into four parts: embankment filling compression, active layer compression, permafrost thawing settlement and warm permafrost compression. The settlement in the first two parts mainly occurred in the first few cycles after the embankment was constructed, and the settlement during railway operation was mainly caused by compression and thawing consolidation of the underlying permafrost (Qi et al., 2007; Qin and Li, 2011). The permafrost beneath the UCRE and CRRE did not thaw (their APTs rose, as shown in Figure 6A) from 2006 to 2018, indicating that embankment settlement does not include thawing settlement in this study. In other words, the compression of permafrost is the main cause for the deformation of the UCRE and CRRE.

The compressibility of permafrost is closely related to temperature and ice content (Zhu and Zhang, 1982; Ladanyi, 1983; Ma et al., 2011). As in the study by French (2007), most ground ice is concentrated in the zone immediately below the PT, as shown in Figure 11. The ice contents of the permafrost underlying the UCRE and CRRE are similar, but the accumulated deformation of the latter is 2.4 times that of the former, as shown in Figure 9A. The reason for this phenomenon is the difference in the permafrost temperature variation beneath the two embankments. First, the thermal regime of high ice content permafrost ( $i > 30\%$ ) is different. At depths of 4.5–8 m, which cover most permafrost layers with high ice contents, the ground temperature beneath the UCRE decreased, with a maximum decrease of  $0.12^{\circ}\text{C}$  (Figure 11A). However, in the high ice content permafrost layer beneath the CRRE, the ground temperature of only the upper 0.5 m thick layer (5–5.5 m depth) slightly decreased, and the decrease was not more than  $0.04^{\circ}\text{C}$ . The temperature of the other 4.2 m (5.5–9.7 m depth) high ice content permafrost increases, with a maximum

increase of  $0.15^{\circ}\text{C}$  (Figure 11B). Second, the warming range of low ice content permafrost ( $i < 30\%$ ) beneath the embankment is also different. The range of temperature increase of permafrost with a low ice content beneath the UCRE is between  $0.03$  and  $0.14^{\circ}\text{C}$ , while that beneath the CRRE is between  $0.17$  and  $0.23^{\circ}\text{C}$  (Figure 11). The cooling of high ice content permafrost and the lesser warming of low ice content permafrost cause compression deformation of warm permafrost beneath the UCRE to be significantly less than that beneath the CRRE, where almost all of the permafrost is significantly warmer. If the average settlement rate of  $1.3$  cm/a from 2016 to 2018 is maintained in the future, the cumulative deformation of the CRRE will exceed the maximum allowable value of  $20$  cm in the China railway design code after 6 years (2024).

According to the above analysis of permafrost degradation rates at different depths and embankment deformation, the stability of the UCRE is significantly better than that of the CRRE. For a period of time in the future, the UCRE can remain stable, but the cooling effect of the crushed-rock revetment structure cannot ensure the stability of the CRRE in warm and ice-rich permafrost regions, which is similar to the conclusions of other studies (Ma et al., 2012; Niu et al., 2015).

## CONCLUSION

Based on ground temperature and deformation data obtained from long-term field monitoring, the stability of two forms crushed-rock embankment under climate warming is evaluated, and the deformation sources are analysed. The following conclusions can be drawn:

- 1) Permafrost, which is affected by climate warming, degrades at both natural sites and crushed-rock structure embankments, but the characteristics of degradation are different. Degradation of permafrost beneath natural sites is manifested by a decrease in thickness and an increase in temperature. The thickness of the permafrost beneath the

embankment increases, but it is degraded, which is manifested by the temperature increase in the deep layer.

- 2) The variation of thermal regime of the shallow permafrost indicates that these two forms crushed-rock structure can slow down the degradation of underlying permafrost in different degrees. The thermal stability of UCRE is better than that of CRRE because more heat is released from UCRE during the cold season due to the convection in the crushed-rock base layer. However, the cooling effect of these two forms of crushed-rock structure began to weaken after 2012 under the influence of climate warming.
- 3) The settlement of the UCRE and CRRE is mainly caused by the compression of underlying warm permafrost. The deformation of the CRRE is 2.4 times greater than that of the UCRE because permafrost degradation is more serious beneath the CRRE, especially in the permafrost layer with a high ice content. The warming of permafrost increases its compressibility and leads to an increase in embankment deformation.
- 4) Under climate warming, the crushed-rock revetment structure can raise the PT beneath the embankment but has little effect on cooling of deep permafrost. Therefore, the CRRE stability of the QTR should be evaluated, and necessary strengthening measures should be taken. U-shaped crushed-rock structures can significantly slow down the warming of the permafrost layer with a high ice content, making the UCRE stable under climate warming. However, it should be noted that permafrost beneath the

UCRE has been in an endothermic state every year for the past 13 years, which requires continuous attention to its future changes.

## DATA AVAILABILITY STATEMENT

The original contributions presented in the study are included in the article/Supplementary Material, further inquiries can be directed to the corresponding author.

## AUTHOR CONTRIBUTIONS

QM: Methodology, writing-original draft, and formal analysis. BY: Visualization, review, and editing. JC: Supervision and funding acquisition. JZ and XH: Data analysis and visualization. YL, JW, SZ, and HD: Data collection, article review, and editing.

## FUNDING

This work was supported by the Strategic Priority Research Program of the Chinese Academy of Science (XDA20020102); the Science and Technology Project of State Grid Corporation of China (SGQHDKYOSBJS201600077); the Natural Science Foundation of China (41101065); and the State Key Laboratory of Frozen Soils Engineering Foundation (SKLFSE-ZT-34).

## REFERENCES

- Cheng, G. (2005). A Roadbed Cooling Approach for the Construction of Qinghai-Tibet Railway. *Cold Regions Sci. Techn.* 42, 169–176. doi:10.1016/j.coldregions.2005.01.002
- Cheng, G., Wu, Q., and Ma, W. (2009). Innovative Designs of Permafrost Roadbed for the Qinghai-Tibet Railway. *Sci. China Ser. E-technol. Sci.* 52, 530–538. doi:10.1007/s11431-008-0291-6
- Ding, Y., Zhang, S., Zhao, L., Li, Z., and Kang, S. (2019). Global Warming Weakening the Inherent Stability of Glaciers and Permafrost. *Sci. Bull.* 64, 245–253. doi:10.1016/j.scib.2018.12.028
- French, H. M. (2007). *The Periglacial Environment*. 3rd ed. Chichester: John Wiley & Sons.
- Goering, D. J., and Kumar, P. (1996). Winter-time Convection in Open-Graded Embankments. *Cold Regions Sci. Techn.* 24, 57–74. doi:10.1016/0165-232X(95)00011-Y
- Goering, D. J. (2003). Passively Cooled Railway Embankments for Use in Permafrost Areas. *J. Cold Reg. Eng.* 17, 119–133. doi:10.1061/(asce)0887-381x(2003)17:3(119)
- Guodong, C., Yuanming, L., Zhizhong, S., and Fan, J. (2007). The 'thermal Semiconductor' Effect of Crushed Rocks. *Permafrost Periglac. Process.* 18, 151–160. doi:10.1002/ppp.575
- He, G. S., Ding, J. k., and Li, Y. Q. (2000). Heat Transmission Properties and Application of the Dump Filling Crushed Stone Layer. *J. Glaciol. Geocryol.* 22, 33–37.
- Hjort, J., Karjalainen, O., Aalto, J., Westermann, S., Romanovsky, V. E., Nelson, F. E., et al. (2018). Degrading Permafrost Puts Arctic Infrastructure at Risk by Mid-century. *Nat. Commun.* 9, 1–9. doi:10.1038/s41467-018-07557-4
- Hong, E., Perkins, R., and Trainor, S. (2014). Thaw Settlement Hazard of Permafrost Related to Climate Warming in Alaska. *Arctic* 67, 93–103. doi:10.14430/arctic4368
- Jilin, Q., Yu, S., Jianming, Z., and Zhi, W. (2007). Settlement of Embankments in Permafrost Regions in the Qinghai-Tibet Plateau. *Norsk Geografisk Tidsskrift - Norwegian J. Geogr.* 61, 49–55. doi:10.1080/00291950701409249
- Jin, H., Wei, Z., Wang, S., Yu, Q., Lü, L., Wu, Q., et al. (2008). Assessment of Frozen-Ground Conditions for Engineering Geology along the Qinghai-Tibet Highway and Railway, China. *Eng. Geology.* 101, 96–109. doi:10.1016/j.enggeo.2008.04.001
- Karjalainen, O., Aalto, J., Luoto, M., Westermann, S., Romanovsky, V. E., Nelson, F. E., et al. (2019). Circumpolar Permafrost Maps and Geohazard Indices for Near-Future Infrastructure Risk Assessments. *Sci. Data* 6, 1–16. doi:10.1038/sdata.2019.37
- Kuang, X., and Jiao, J. J. (2016). Review on Climate Change on the Tibetan Plateau during the Last Half century. *J. Geophys. Res. Atmos.* 121, 3979–4007. doi:10.1002/2015JD024728
- Ladanyi, B. (1983). Shallow Foundations on Frozen Soil: Creep Settlement. *J. Geotechnical Eng.* 109, 1434–1448. doi:10.1061/(asce)0733-9410(1983)109:11(1434)
- Lai, Y., Pei, W., and Yu, W. (2014). Calculation Theories and Analysis Methods of Thermodynamic Stability of Embankment Engineering in Cold Regions. *Chin. Sci. Bull.* 59, 261–272. doi:10.1007/s11434-013-0012-9
- Lai, Y., Zhang, L. X., Zhang, S. J., and Mi, L. (2003). Cooling Effect of Ripped-Stone Embankments on Qing-Tibet Railway under Climatic Warming. *Chin. Sci Bull* 48, 598–604. doi:10.1360/03tb9127
- Lai, Y., Zhang, M., Liu, Z., and Yu, W. (2006). Numerical Analysis for Cooling Effect of Open Boundary Ripped-Rock Embankment on Qinghai-Tibetan Railway. *Sci. China Ser. D* 49, 764–772. doi:10.1007/s11430-006-0764-z
- Li, R., Wu, Q., Li, X., Sheng, Y., Hu, G., Cheng, G., et al. (2019). Characteristic, Changes and Impacts of Permafrost on Qinghai-Tibet Plateau. *Chin. Sci. Bull.* 64, 2783–2795. doi:10.1360/tb-2019-0191
- Liu, J., Tai, B., and Fang, J. (2019). Ground Temperature and Deformation Analysis for an Expressway Embankment in Warm Permafrost Regions of the Tibet Plateau. *Permafrost and Periglac Process* 30, 208–221. doi:10.1002/ppp.2007
- Luo, J., Niu, F., Liu, M., Lin, Z., and Yin, G. (2018). Field Experimental Study on Long-Term Cooling and Deformation Characteristics of Crushed-Rock Revetment Embankment at the Qinghai-Tibet Railway. *Appl. Therm. Eng.* 139, 256–263. doi:10.1016/j.applthermaleng.2018.04.138

- Ma, W., Cheng, G.-d., Wu, Q.-b., and Wang, D.-y. (2005). Application on Idea of Dynamic Design in Qinghai-Tibet Railway Construction. *Cold Regions Sci. Techn.* 41, 165–173. doi:10.1016/j.coldregions.2004.09.002
- Ma, W., Feng, G., Wu, Q., and Wu, J. (2008a). Analyses of Temperature fields under the Embankment with Crushed-Rock Structures along the Qinghai-Tibet Railway. *Cold Regions Sci. Techn.* 53, 259–270. doi:10.1016/j.coldregions.2007.08.001
- Ma, W., Mu, Y., Wu, Q., Sun, Z., and Liu, Y. (2011). Characteristics and Mechanisms of Embankment Deformation along the Qinghai-Tibet Railway in Permafrost Regions. *Cold Regions Sci. Techn.* 67, 178–186. doi:10.1016/j.coldregions.2011.02.010
- Ma, W., Mu, Y., Zhang, J., Yu, W., Zhou, Z., and Chen, T. (2019). Lateral thermal Influences of Roadway and Railway Embankments in Permafrost Zones along the Qinghai-Tibet Engineering Corridor. *Transportation Geotechnics* 21, 100285. doi:10.1016/j.trgeo.2019.100285
- Ma, W., Qi, J., and Wu, Q. (2008b). Analysis of the Deformation of Embankments on the Qinghai-Tibet Railway. *J. Geotech. Geoenviron. Eng.* 134, 1645–1654. doi:10.1061/(asce)1090-0241(2008)134:11(1645)
- Ma, W., Wen, Z., Sheng, Y., Wu, Q., Wang, D., and Feng, W. (2012). Remedying Embankment Thaw Settlement in a Warm Permafrost Region with Thermosyphons and Crushed Rock Revetment. *Can. Geotech. J.* 49, 1005–1014. doi:10.1139/T2012-058
- Mei, Q.-H., Chen, J., Wang, J.-C., Hou, X., Zhao, J.-Y., Zhang, S.-H., et al. (2021). Strengthening Effect of Crushed Rock Revetment and Thermosyphons in a Traditional Embankment in Permafrost Regions under Warming Climate. *Adv. Clim. Change Res.* 12, 66–75. doi:10.1016/j.accre.2021.01.002
- Mu, Y. H., Ma, W., Niu, F. J., Liu, Y. Z., Fortier, R., and Mao, Y. C. (2018). Long-term thermal Effects of Air Convection Embankments in Permafrost Zones: Case Study of the Qinghai-Tibet Railway, China. *J. Cold Reg. Eng.* 32, 1–10. doi:10.1061/(ASCE)CR.1943-5495.0000166
- Mu, Y. H. (2012). “Analyses on Dynamic Variations of Embankment Thermal Regime and Deformation along the Qinghai-Tibet Railway in Permafrost Regions.” ([Lanzhou]: Chinese Academy of Sciences). PHD thesis.
- Mu, Y., Ma, W., Liu, Y., and Sun, Z. (2010). Monitoring Investigation on thermal Stability of Air-Convection Crushed-Rock Embankment. *Cold Regions Sci. Techn.* 62, 160–172. doi:10.1016/j.coldregions.2010.03.007
- Nelson, F. E., Anisimov, O. A., and Shiklomanov, N. I. (2001). Subsidence Risk from Thawing Permafrost. *Nature* 410, 889–890. doi:10.1038/35073746
- Niu, F., Liu, M., Cheng, G., Lin, Z., Luo, J., and Yin, G. (2015). Long-term thermal Regimes of the Qinghai-Tibet Railway Embankments in Plateau Permafrost Regions. *Sci. China Earth Sci.* 58, 1669–1676. doi:10.1007/s11430-015-5063-0
- Peng, H., Ma, W., Mu, Y.-h., and Jin, L. (2015). Impact of Permafrost Degradation on Embankment Deformation of Qinghai-Tibet Highway in Permafrost Regions. *J. Cent. South. Univ.* 22, 1079–1086. doi:10.1007/s11771-015-2619-2
- Qin, Y., and Li, G. (2011). Permafrost Warming under the Earthen Roadbed of the Qinghai-Tibet Railway. *Environ. Earth Sci.* 64, 1975–1983. doi:10.1007/s12665-011-1014-z
- Streletskiy, D. A., Suter, L. J., Shiklomanov, N. I., Porfiriev, B. N., and Eliseev, D. O. (2019). Assessment of Climate Change Impacts on Buildings, Structures and Infrastructure in the Russian Regions on Permafrost. *Environ. Res. Lett.* 14, 025003. doi:10.1088/1748-9326/aaf5e6
- Sun, Z. Z., Ma, W., Zhang, S. J., Wen, Z., and Wu, G. L. (2018). Embankment Stability of the Qinghai-Tibet Railway in Permafrost Regions. *J. Cold. Reg. Eng.* 32, 1–7. doi:10.1061/(ASCE)CR.1943-5495.0000153
- Tai, B., Wu, Q., Zhang, Z., and Xu, X. (2020). Cooling Performance and Deformation Behavior of Crushed-Rock Embankments on the Qinghai-Tibet Railway in Permafrost Regions. *Eng. Geology.* 265, 105453. doi:10.1016/j.enggeo.2019.105453
- Tong, C. J., and Wu, Q. B. (1996). The Effect of Climate Warming on the Qinghai-Tibet Highway, China. *Cold Reg. Sci. Technol.* 24, 101–106. doi:10.1016/0165-232X(95)00012-Z
- Wei, M., Guodong, C., and Qingbai, W. (2009). Construction on Permafrost Foundations: Lessons Learned from the Qinghai-Tibet railroad. *Cold Regions Sci. Techn.* 59, 3–11. doi:10.1016/j.coldregions.2009.07.007
- Wu, Q. B., Cheng, G. D., Ma, W., Niu, F., and Sun, Z. Z. (2006). Technical Approaches on Permafrost thermal Stability for Qinghai-Tibet Railway. *Geomechanics and Geoengineering* 1, 119–127. doi:10.1080/17486020600777861
- Wu, Q., Dong, X., Liu, Y., and Jin, H. (2007). Responses of Permafrost on the Qinghai-Tibet Plateau, China, to Climate Change and Engineering Construction. *Arctic, Antarctic, Alpine Res.* 39, 682–687. doi:10.1657/1523-0430(07-508)[wu]2.0.co;2
- Wu, Q., Hou, Y., Yun, H., and Liu, Y. (2015). Changes in Active-Layer Thickness and Near-Surface Permafrost between 2002 and 2012 in alpine Ecosystems, Qinghai-Xizang (Tibet) Plateau, China. *Glob. Planet. Change* 124, 149–155. doi:10.1016/j.gloplacha.2014.09.002
- Wu, Q., Lu, Z., Tingjun, Z., Ma, W., and Liu, Y. (2008). Analysis of Cooling Effect of Crushed Rock-Based Embankment of the Qinghai-Xizang Railway. *Cold Regions Sci. Techn.* 53, 271–282. doi:10.1016/j.coldregions.2007.10.004
- Wu, Q., and Niu, F. (2013). Permafrost Changes and Engineering Stability in Qinghai-Xizang Plateau. *Chin. Sci. Bull.* 58, 1079–1094. doi:10.1007/s11434-012-5587-z
- Wu, Q., Sheng, Y., Yu, Q., Chen, J., and Ma, W. (2020a). Engineering in the Rugged Permafrost Terrain on the Roof of the World under a Warming Climate. *Permafrost and Periglacial Process* 31, 417–428. doi:10.1002/ppp.2059
- Wu, Q., Shi, B., and Fang, H.-Y. (2003). Engineering Geological Characteristics and Processes of Permafrost along the Qinghai-Xizang (Tibet) Highway. *Eng. Geology.* 68, 387–396. doi:10.1016/S0013-7952(02)00242-9
- Wu, Q., Zhang, T., and Liu, Y. (2012). Thermal State of the Active Layer and Permafrost along the Qinghai-Xizang (Tibet) Railway from 2006 to 2010. *The Cryosphere* 6, 607–612. doi:10.5194/tc-6-607-2012
- Wu, Q., Zhao, H., Zhang, Z., Chen, J., and Liu, Y. (2020b). Long-term Role of Cooling the Underlying Permafrost of the Crushed Rock Structure Embankment along the Qinghai-Xizang Railway. *Permafrost and Periglacial Process* 31, 172–183. doi:10.1002/ppp.2027
- Xu, X. Z., Wang, J. C., and Zhang, L. X. (2010). *Physics of Frozen Soils*. Beijing: Science Press.
- Yandong, H., Qingbai, W., Yongzhi, L., Zhongqiong, Z., and Siru, G. (2015). The thermal Effect of Strengthening Measures in an Insulated Embankment in a Permafrost Region. *Cold Regions Sci. Techn.* 116, 49–55. doi:10.1016/j.coldregions.2015.04.003
- Zhang, J. M., Liu, D., and Qi, J. L. (2007). Estimation on the Settlement and Deformation of Embankment along Qinghai-Tibet Railway in Permafrost Regions. *Chin. Rail. Sci.* 25, 12–17. doi:10.1364/AO.46.001107
- Zhang, T., Baker, T. H. W., Cheng, G.-D., and Wu, Q. (2008). The Qinghai-Tibet Railroad: A Milestone Project and its Environmental Impact. *Cold Regions Sci. Techn.* 53, 229–240. doi:10.1016/j.coldregions.2008.06.003
- Zhao, H., Wu, Q., and Zhang, Z. (2019). Long-term Cooling Effect of the Crushed Rock Structure Embankments of the Qinghai-Tibet Railway. *Cold Regions Sci. Techn.* 160, 21–30. doi:10.1016/j.coldregions.2019.01.006
- Zhongqiong, Z., Qingbai, W., Guanli, J., Siru, G., Ji, C., and Yongzhi, L. (2020). Changes in the Permafrost Temperatures from 2003 to 2015 in the Qinghai-Tibet Plateau. *Cold Regions Sci. Techn.* 169, 102904. doi:10.1016/j.coldregions.2019.102904
- Zhu, Y. L., and Zhang, J. Y. (1982). Elastic and Compressive Deformation of Frozen Soils. *Chin. J. Glaciol. Geocryol* 4, 29–40.

**Conflict of Interest:** YL, JW, SZ, and HD were employed by China Railway Qinghai-Tibet Group Co., Ltd.

The remaining authors declare that the research was conducted in the absence of any commercial or financial relationships that could be construed as a potential conflict of interest.

**Publisher’s Note:** All claims expressed in this article are solely those of the authors and do not necessarily represent those of their affiliated organizations, or those of the publisher, the editors and the reviewers. Any product that may be evaluated in this article, or claim that may be made by its manufacturer, is not guaranteed or endorsed by the publisher.

Copyright © 2021 Mei, Yang, Chen, Zhao, Hou, Liu, Wang, Zhang and Dang. This is an open-access article distributed under the terms of the Creative Commons Attribution License (CC BY). The use, distribution or reproduction in other forums is permitted, provided the original author(s) and the copyright owner(s) are credited and that the original publication in this journal is cited, in accordance with accepted academic practice. No use, distribution or reproduction is permitted which does not comply with these terms.

## NOMENCLATURE

**(A)PT**, (artificial) permafrost table;

**CRREs**, crushed-rock revetment embankments;

**MAGT**, mean annual ground temperature;

**QTP**, Qinghai-Tibetan Plateau;

**QTR**, Qinghai-Tibet Railway;

**UCREs**, U-shaped crushed-rock embankments